Turkish Online Journal of Qualitative Inquiry (TOJQI)
Volume 11, Issue 4, December 2020: 2745 -2758
DOI: 10.53555/tojqi.v11i4.10358

Research Article

Evaluation of Photophysical Properties of Biological Active 3-(2-(1H-Imidazol-1-Yl)-1-Methoxyethyl)-2H-Chromen-2-One Derivatives Using Density Functional Theory

Kasala Suresha[1], A. Anthony Seleen[2], Rashmi D[3], Anil Kumar[4], Kavitha B. S[5*]

Abstract

This research delves into Density Functional Theory (DFT) investigations concerning a novel 1-Aza-Coumarin-Linked Miconazole derivative, denoted as 4-((2-(1H-benzo[d]imidazol-1-yl)-1-(2-oxo-2H-chromen-3-yl)ethoxy)methyl)-7-methoxy-2H-chromen-2-one (4BEXO). Utilizing DFT calculations, we examined various energy components of 4BEXO in its ground state, both in isolation and in diverse solvent environments, to analyze solvent effects comprehensively. Through computational analysis, the bond lengths, angles, and dihedral angles suggest that the molecule possesses a stable configuration, optimized for minimal strain and favorable electronic distribution. The Mulliken charge distribution indicates a shift in electron density when the molecule is placed in different solvents, highlighting the influence of the surrounding environment on its reactivity and stability. Furthermore, the Global Chemical Reactivity Descriptors (GCRD) reveal a balance between stability and reactivity, with the HOMO-LUMO energy gap (3.726 eV) suggesting moderate chemical stability with potential for reactivity. The ionization potential (6.413 eV) and electron affinity (2.687 eV) indicate that the molecule has a moderate tendency to lose and gain electrons, respectively. The chemical hardness (1.863 eV) and softness (0.268 eV^{-1}) values reflect a relatively stable yet reactive nature, with a high electrophilicity index (5.556 eV) confirming the molecule's strong electrophilic character. Our analysis encompassed optimized geometry, Mulliken charge distribution in ground and excited states, and computed highest occupied molecular orbital and lowest unoccupied molecular orbital gaps of 4BEXO in different mediums, facilitating the determination of solvation energy, ionization potential, electron affinity, chemical hardness, electron chemical potential, electronegativity, and global electrophilicity. Additionally, we scrutinized UV-Vis spectrum and emission energy using the Time-Dependent DFT (TD-DFT) method, and conducted density distribution analysis via total electron density and molecular electrostatic potential to comprehend potential distribution across the molecule. Furthermore, a frontier molecular orbitals analysis was undertaken. This study aims to provide insights into the electronic, thermodynamic, and spectroscopic parameters of the coumarin derivative, particularly considering solvent and solute-solvent interactions. Overall, these findings suggest that 4BEXO is a stable yet reactive compound, with potential applications in fields requiring specific interactions with nucleophiles and other reactive species.

Keywords: DFT, Mulliken, UV-Vis, MESP, FMO.

[1]Department of Physics, Government First Grade College, Hosadurga-577527, India
[2]Department of Physics, Government First Grade College, Chamarajanagar-571313, Karnataka India
[3]Department of Biochemistry, Maharani Science College for Women, Palace Road, Bangalore-560001, Karnataka India
[4]P.G. Department of Physics, Shri Siddeshwar Government First Grade College, Naragund - 582207, Karnataka India
[5]Department of Physics, Government First Grade College, Tiptur- 572201, Karnataka India. Email id:kavitha.samu@gmail.com

1. Introduction

Coumarin and its derivatives are a highly versatile class of compounds known for their broad range of biological activities [1]. These compounds have demonstrated effectiveness as antibacterial, antifungal, anti-inflammatory, anticoagulant, anti-HIV, and antitumor agents. They are widely utilized in various industries, including food, perfumes, cosmetics, pharmaceuticals, and as optical brighteners [2-6]. Due to their excellent thermal stability and remarkable optical properties, such as broad spectral response, high quantum yields, and superior photostability, coumarins are extensively studied for optical applications. These applications include their use as laser dyes, nonlinear optical chromophores, fluorescent whiteners, probes, polymer science, optical recording, and solar energy collection [7-8].

Traditionally, coumarins are synthesized through several key reactions, including Pechmann, Knoevenagel, Perkin, Reformatsky, and Wittig condensations. Various modifications in catalysts and reaction conditions have been introduced to enhance the efficiency of these classical reactions [9]. Among coumarin derivatives, 4-hydroxycoumarin is particularly notable for its anticoagulant properties, making it useful in treating conditions like thrombophlebitis, pulmonary embolism, and certain heart conditions. Comparative pharmacological studies have shown that 4-hydroxycoumarin derivatives offer effective anticoagulant activity with minimal side effects and low toxicity[10].

Antioxidants, including those found in coumarin derivatives, play a vital role in protecting cellular components from oxidative stress caused by free radicals [11]. These free radicals, such as hydroxyl radicals, superoxide anions, and hydrogen peroxide, can damage biomolecules and contribute to diseases like cancer, coronary heart disease, and hypertension. Although the body's endogenous defense systems, such as catalase, superoxide dismutase, and the peroxidase–glutathione system, generally counteract free radicals, coumarins' antioxidant properties provide additional protection [12-15].

In view of the above discussion, in the present work4-((2-(1H-benzo[d]imidazol-1-yl)-1-(2-oxo-2H-chromen-3-yl)ethoxy)methyl)-7-methoxy-2H-chromen-2-one(4BEXO) is selected and studied the their photophysical and chemical properties using DFT method.

2. Computational techniques

The 1-Aza-Coumarin-Linked Miconazole derivatives, namely4-((2-(1H-benzo[d]imidazol-1-yl)-1-(2-oxo-2H-chromen-3-yl)ethoxy)methyl)-7-methoxy-2H-chromen-2-one(4BEXO) is selected from the literature [16] and the molecular structure of the 4BEXO was given in Figure-1.

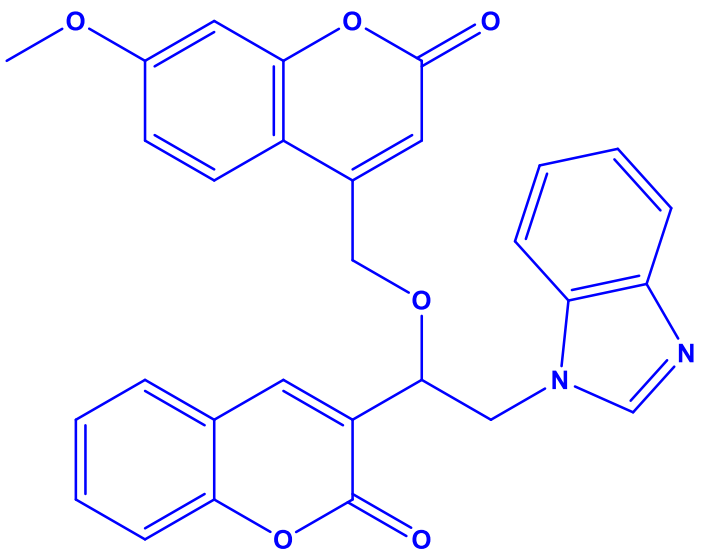

Figure-1 Molecular structure of the 4BEXO molecule

The structural and theoretical analyses of 4BEXO were conducted using the GaussView 5.0 and Gaussian 09W software packages [17]. The optimization of 4BEXO geometry was initially performed via Density Functional Theory (DFT) employing the B3LYP functional and the 6-311G** basis set. Subsequently, various theoretical investigations were carried out, encompassing atomic charge distribution in the ground state, Time-Dependent DFT (TD-DFT) analysis in the excited state, thermodynamic properties, structural properties, and optical properties. The DFT method B3LYP/6-311G** was utilized for these analyses. Additionally, frontier molecular orbital analysis of the molecule was conducted both in vacuum and in a liquid-phase environment. This comprehensive approach enabled a thorough exploration of 4BEXO's electronic structure, thermodynamic behavior, and optical characteristics, shedding light on its potential applications and informing further research endeavors.

Thermodynamic parameters including Self-Consistent Field (SCF) energy, enthalpy, entropy, dipole moment, zero-point vibrational energy, heat capacity, and rotational constants were computed to elucidate 4BEXO's energetic and structural attributes. Furthermore, UV-Vis and emission spectroscopy analyses were performed on 4BEXO in various media, utilizing Time-Dependent Density Functional Theory (TD-DFT) at the B3LYP/6-311G** level. This provided insights into the molecule's electronic transitions and oscillatory strengths under different environmental conditions. Moreover, the energy levels of the HOMO and LUMO were examined across different mediums, allowing for the assessment of key molecular properties such as ionization potential, electron affinity, chemical hardness, and electrophilicity index. Additionally, Density Functional Theory (DFT) was employed to analyze the Total Electron Density (TED) surface mapping, Electrostatic Potential (ESP), and Molecular Electrostatic Potential (MEP) contour mapping of 4BEXO in both vacuum and solvent mediums, offering insights into its molecular interactions.

3. Results and discussion

3.1. Structure and geometric propertiesof 4BEXO

The structural design of 4BEXO was initially generated in GaussView-5 and subsequently optimized using Gaussian 09 software. The optimization process, conducted with the "opt" keyword, utilized the B3LYP functional and the 6-311G basis set [18]. Starting from standard parameters, the Gaussian program iteratively minimized the geometry to identify the configuration with the lowest energy, resembling the molecular structure at its energy minimum. The resulting optimized molecular geometries of 4BEXO are depicted in Figure-2, providing visual representation of the molecule's conformational characteristics.

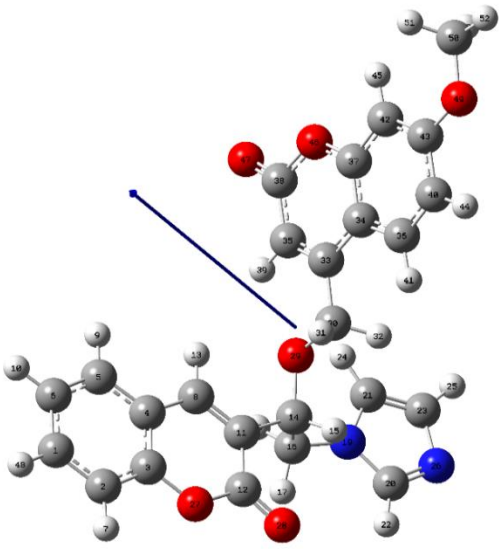

Figure-2 Optimised molecular geometry of the 4BEXO molecule

The bond lengths, bond angles, and dihedral angles of the molecule 4BEXO are given in Table -1. The C-C bond lengths within the aromatic rings, such as C1-C2 and C2-C3, are around 1.392 Å, reflecting good aromatic stability, while slightly longer single bonds, such as C11-C14 (1.516 Å) and C14-C16 (1.539 Å), suggest some flexibility in the structure. The C-O bond lengths, particularly the short C12-O28 bond (1.232 Å), indicate strong, stable carbonyl and ether bonds, contributing to the rigidity of the molecule in those regions. The bond angles further support this stability, with angles like C1-C2-C3 (118.61°) and C2-C3-O27 (117.66°) closely aligning with ideal sp^2 hybridized carbon angles, minimizing strain within the aromatic systems. However, slight deviations, such as the C16-N19-C21 angle (127.07°), suggest some strain in the imidazole ring, which could affect stability but may enhance the molecule's reactivity. Tetrahedral angles around the carbonyl group, such as O29-C30-C33 (109.89°), reinforce the stability of the ether and chromen groups. The dihedral angles reveal the presence of torsional strain, indicating that certain sections of the molecule are not entirely planar. For example, the C12-C11-C14-C16 (75.65°) and H17-C16-N19-C21 (159.40° and 41.20°) angles suggest flexibility, which could reduce conjugation between different parts of the molecule. However, this flexibility might also enhance the molecule's adaptability in different environments, potentially aiding in biological interactions.

Overall, the molecule exhibits a stable structure with well-optimized bond lengths and angles, despite some torsional strain. This balance between rigidity and flexibility suggests that the molecule is structurally sound while remaining versatile and reactive, making it potentially effective in various applications.[19].

Table-1 Estimation of Bondlength(Å),Bondangle(°)and dihedralangleof4BEXOusingDFT/B3LYP/6-311G

Atoms	Bond length(Å)	Atoms	Bond Angle (°)	Atoms	Dihedral Angle(°)
C1-H48	1.081	C1-C2-C3	118.61	C12-C11-C14-C16	75.65
C1-C2	1.392	C2-C3-O27	117.66	C11-C14-C16-H18	7058
C2-C3	1.392	C3-O27-C12	122.58	H17-C16-N19-C21	159.40
C3-O27	1.393	O27-C12-O28	117.92	H18-C16-N19-C21	41.20
O27-C12	1.413	O28-C12-C11	125.53	C14-O29-C30-H32	65.01
C12-O28	1.232	C11-C14-C16	112.36	H32-C30-C33-C35	122.30
C12-C11	1.457	C14-C16-N19	112.58	H51-C50-O49-C43	61.73
C11-C14	1.516	C16-N19-C21	127.07		
C14-C16	1.539	C14-O29-C30	115.02		
C16-N19	1.457	O29-C30-C33	109.89		
N19-C21	1.394	H31-C30-H32	107.99		
C21-C23	1.373	C43-O49-C50	119.35		
C23-N26	1.396				
N26-C20	1.327				
C20-N19	1.327				
C14-O29	1.459				
O29-C30	1.452				
C30-C33	1.506				
O47-C38	1.227				
O46-C38	1.432				
O46-C37	1.387				
C43-O49	1.381				
O49-C50	1.452				

The Mulliken atomic charge distributions [20] of each atomic site in 4BEXO were investigated using DFT with the B3LYP/6-311Gmethod in three different environments: vacuum, hexene, and dimethyl sulfoxide solvents (DMSO). Table-2 presents the Mulliken charge distribution of each atom in 4BEXOdifferent mediums, highlighting the solvent influences.The Figure-3 and 4 werethe shows, the graphically illustrates of the variation in charge distribution acrossmolecules. The

Mulliken charge distribution of the molecule 4BEXO across different solvents (vacuum, hexene, and DMSO) reveals significant variations in electron density, which affect the molecule's reactivity and stability. In a vacuum, the molecule displays a higher degree of polarization, with more pronounced positive and negative charges on specific atoms. This suggests that without a solvent to stabilize the charge distribution, the molecule is more reactive and susceptible to nucleophilic or electrophilic attacks.

In contrast, in the polar solvent DMSO, the charges on many atoms become more neutral, indicating that the solvent stabilizes the electron distribution by reducing polarization. This stabilization by DMSO suggests that the molecule is less reactive but more stable in such an environment. Hexene, being a non-polar solvent, exhibits intermediate behavior, where the molecule's charges are somewhat stabilized but not as effectively as in DMSO.

Key atoms such as oxygen and nitrogen show significant reductions in their negative charges in DMSO compared to vacuum, highlighting the solvent's ability to stabilize lone pairs and reduce the molecule's overall reactivity. Additionally, carbon atoms connected to electronegative atoms exhibit higher positive charges in DMSO, indicating enhanced electron withdrawal in a polar environment. Overall, the Mulliken charge distribution indicates that the choice of solvent profoundly influences the molecule's stability and reactivity. In polar solvents like DMSO, the molecule is more stable but less reactive, making it suitable for applications requiring stability. In non-polar solvents or vacuum, the molecule retains higher reactivity, which may be desirable in certain chemical reactions.

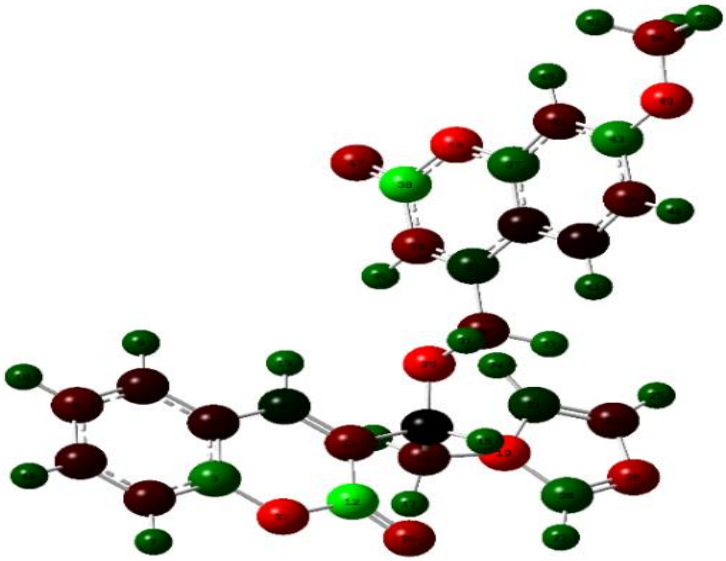

Figure-3 Mulliken charge distribution on the 4BEXO molecule

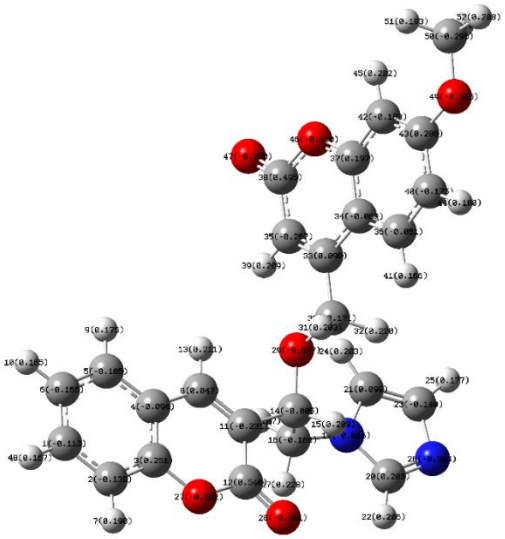

Figure-4 Statistical representation of Mulliken charge distribution on the4BEXO molecule in gas phase

Table-2 Mulliken atomic charges by DFT/ B3LYP/6-311G in vacuum and solvent medium

Atom label	Vacuum	Hexene	DMSO
1C	-0.113	0.025	0.035
2C	-0.138	0.000	0.010
3C	0.251	0.389	0.399
4C	-0.095	0.043	0.053
5C	-0.105	0.033	0.043
6C	-0.165	-0.027	-0.017
7H	0.191	0.329	0.339
8C	0.048	0.186	0.196
9H	0.176	0.314	0.324
10H	0.166	0.304	0.314
11C	-0.229	-0.091	-0.081
12C	0.541	0.679	0.689
13H	0.211	0.349	0.359
14H	-0.006	0.132	0.142
15H	0.209	0.347	0.357
16C	-0.168	-0.030	-0.020
17H	0.229	0.367	0.377
18H	0.208	0.346	0.356
19N	-0.626	-0.488	-0.478
20C	0.203	0.341	0.351
21C	0.098	0.236	0.246
22H	0.207	0.345	0.355
23C	-0.140	-0.002	0.008
24H	0.203	0.341	0.351
25H	0.177	0.315	0.325
26N	-0.369	-0.231	-0.221
27O	-0.501	-0.363	-0.353
28O	-0.362	-0.224	-0.214
29O	-0.528	-0.390	-0.380
30C	-0.169	-0.031	-0.021
31H	0.205	0.343	0.353
32H	0.220	0.358	0.368
33C	0.088	0.226	0.236
34C	-0.075	0.063	0.073
35C	-0.263	-0.125	-0.115

36C	-0.045	0.093	0.103
37C	0.224	0.362	0.372
38C	0.498	0.636	0.646
39H	0.212	0.350	0.360
40C	-0.163	-0.025	-0.015
41H	0.170	0.308	0.318
42C	-0.168	-0.030	-0.020
43C	0.274	0.412	0.422
44H	0.168	0.306	0.316
45H	0.196	0.334	0.344
46O	-0.507	-0.369	-0.359
47O	-0.346	-0.208	-0.198
48H	0.167	0.305	0.315
49O	-0.512	-0.374	-0.364
50C	-0.311	-0.173	-0.163
51H	0.186	0.324	0.334
52H	0.200	0.338	0.348
53H	0.181	0.319	0.329

The thermodynamic parameters serve as pivotal indicators in understanding chemical processes. Utilizing Density Functional Theory (DFT), we investigated various statistical thermodynamic properties of 4BEXO at a temperature of 298.15 K and 1atm pressure. The DFT/B3LYP/6-311G method facilitated the determination of translational, rotational, vibrational, total, and nuclear repulsion energies, as well as zero-point vibrational energy and other statistical thermodynamic parameters such as entropy (S), rotational constants, molecular capacity at constant volume, and dipole moment. These findings, outlined in Table 3, provide essential insights for further exploration of 4BEXO's molecular behavior and pave the way for comprehensive studies on this compound [21].

Table-3 Calculated thermodynamic parameters of 4BEXO with DFT theory using the B3LYP/6-311G (d, p) basis set

Parameters	Values
Energy	
Translational(kcalmol^{-1})	0.892
Rotational(kcalmol^{-1})	0.892
Vibrational(kcalmol^{-1})	97.072
Total	98.756
Nuclear repulsion energy (Hartree's)	1079
Zero-point vibrational energy(kcalmol^{-1})	116.009
Entropy,S(Cal/Mol-Kelvin)	118.083
Molecular capacity of constant volume (cal mol^{-1} k^{-1})	4.284
Translational	1.554
Rotational	38.212
Vibrational	49.222
Total	
Rotationalconstants(GHz)	
A	1.132
B	0.199
C	0.121
Dipole moment (D)	9.932

The TD-DFT method has been used to discover the UV-Visible spectra of 4BEXO in vacuum, hexene, and DMSO medium, as shown in Figure 5. Results related to the vertical excitation energies, oscillator strength (f), and wavelength have been obtained. The TD-DFT has been employed to examine the absorption spectra with an efficient approach [21]. The TD-DFT calculation predicts an intense digital transition at 342 nm with an oscillator strength (f) of 0.398 in vacuum, at 344 nm with f = 0.412 in hexene, and at 352 nm with f = 0.431 in DMSO, as shown in Figure 5. The estimation of fluorescence access using the TD-DFT approach involves optimizing the electronically excited-state (EES) geometry, its vertical energies (absorption or emission), and the measured longest wavelength of absorption (λ_max) through an approximated procedure [22]. Observations from Figure 5 reveal a red shift in the absorption spectra of the 4BEXO molecule, suggesting its high polarity in the excited state. This finding is confirmed by the significant dipole moment obtained from TD-DFT methods.

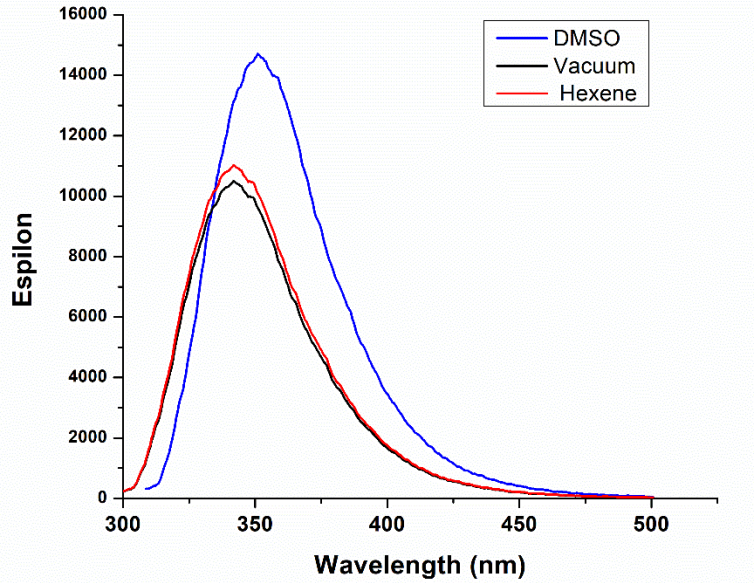

Figure-5 Absorption spectra of 4BEXO in different media estimated using TD-DFTanalysis

3.2. Frontier Molecular Orbitals (FMO) and Quantum chemical calculation

The FMO enables to recognize the electron charge transfer between the donor and acceptor group by the π-conjugate. The HOMO (electron-donating) directly associated with the ionization potential, even as the LUMO (electron-accepting) associated with the electron affinity of the compound. Plot of FMO helps us to have higher information of the nature of the chemical structure and chemical reaction of the molecule [9, 22]. HOMO, HOMO-1, HOMO-2 are the orbitals that present π-bonding symmetry and LUMO, LUMO+1, LUMO+2 are molecular orbitals that shows π* antibonding symmetry. Figure-6 indicates a 3D representation of frontier molecular orbital in different medium using DFT method with B3LYP functional and 6-311G basis set in which greenish area indicates the positive region and reddish area shows the negative region of the molecular orbital.

The energy gap (E_g) has been analysed using the equation (1) given below, which gives energy gap (E_g) between HOMO to LUMO. The E_g shows the largest energy gap of 3.726eV, energy gap of HOMO-1 to LUMO+1 is 4.344 eV and the E_g between HOMO+2 to LUMO-2 is 5.572eV.

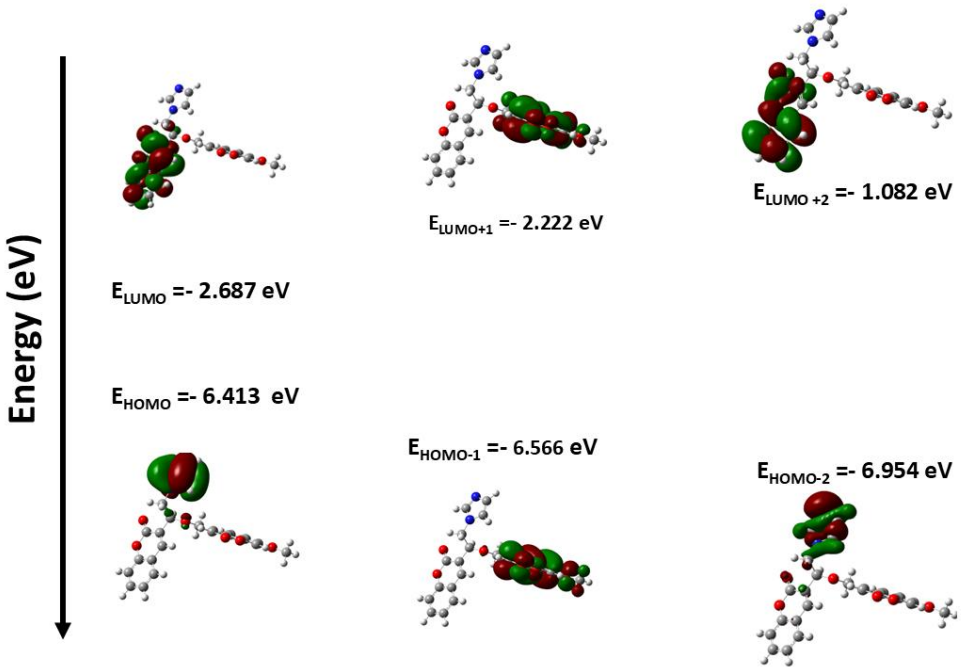

Figure-6 3 D representation of frontier molecular orbital of 4BEXO in vacuum using DFT method.

It is important to study the global chemical reactivity descriptors (GCRD) properties [23] to understand more about the stability and reactivity of synthesized compounds. The GCRD parameters like chemical hardness ($\eta = (IP - EA)/2$), electronegativity ($\chi = (IP + EA)/2$), chemical potential ($\mu = -\chi$), chemical softness ($S = 1/2\eta$) and electrophilicity index ($\omega = \mu^2/2\eta$) were calculated from E_{HOMO} and E_{LUMO} values, where, ionization potential, $IP = -E_{HOMO}$ and electron affinity, $EA = -E_{LUMO}$.

From Figure-6 it is observed that LUMO electron cloud mainly distribute across the coumarin molecule and HOMO electron cloud partially located on the 1-methyl-1H-imidazole. The GCRD parameters of all the molecules are given in Table 6. It is noticed that, the designed compounds with different position groups show different energy gaps. The HOMO energy (E_{HOMO}) is -6.413 eV, indicating that the molecule is relatively stable and does not easily donate electrons, which suggests it has moderate nucleophilic behavior. The LUMO energy (E_{LUMO}) is -2.687 eV, indicating a decent ability to accept electrons and suggesting the molecule can act as an electrophile. The energy gap (ΔE) between HOMO and LUMO is 3.726 eV, reflecting a balance between stability and reactivity, making the molecule suitable for applications requiring moderate stability with some reactivity.

The ionization potential (IP) is 6.413 eV, which indicates that the molecule is relatively stable and resistant to losing an electron. The electron affinity (EA) is 2.687 eV, suggesting that the molecule has a decent capacity to gain electrons, further supporting its electrophilic nature. The chemical hardness (η) is 1.863 eV, which implies that the molecule is moderately stable and resistant to changes in its electron distribution, while the electronegativity (χ) of 4.550 eV reflects a moderate tendency to attract electrons.

The chemical potential (μ) is -4.550 eV, indicating that the molecule prefers to retain its electrons, contributing to its stability. The softness (s) value of 0.268 eV^{-1} suggests that the molecule is relatively hard and resistant to electron cloud deformation. Finally, the electrophilicity index (ω) of 5.556 eV suggests that the molecule is a strong electrophile, making it particularly reactive toward nucleophiles.

The GCRD parameters indicate that this molecule is relatively stable with a balanced ability to donate and accept electrons. Its moderate hardness and high electrophilicity make it a potentially reactive species in chemical reactions, particularly in scenarios where both nucleophilic and electrophilic behaviors are advantageous.

Table-4 Global electrochemical reactivity descriptor parameter for all synthesized molecules

E_{HOMO} (eV)	E_{LUMO} (eV)	ΔE (eV)	IP (eV)	EA (eV)	η (eV)	χ (eV)	μ (eV)	s (eV^{-1})	ω (eV)
–6.413	–2.687	3.726	6.413	2.687	1.863	4.550	-4.550	0.268	5.556

3.3. Electrostatic potential (ESP), total electron density (TED) and molecular electrostatic potential (MESP) studies

Three-dimensional mappings of electrostatic potential, total electron density, and molecular electrostatic potential were generated using DFT theory with the B3LYP functional and 6-311+G (d,p) basic set. These mappings of3-(2-(1H-Imidazol-1-Yl)-1-Methoxyethyl)-2H-Chromen-2-One structures was analysed through surface contouring in Gaussian-09W.

3.3.1. ESP of 4BEXO molecule

The electrostatic Potential (ESP) illustrates the interaction energy between the molecule's electrons and point positive charges near nuclei. Figure-7 displays the ESP mapping of the 4BEXO molecule, indicating energy ranging from -0.587 eV to 0.587 eV in vacuum and from -0.677 eV to 0.677 eV in DMSO solvent. Notably, sites O22 and O23 exhibit the most negative potential values of -0.342 eV and -0.342 eV, respectively, in vacuumand these areas are highlighted in red. Additionally, the region encompassing 14N and 21N shows potential values of 0.432 eV and 0.165 eV (yellow) in vacuum.

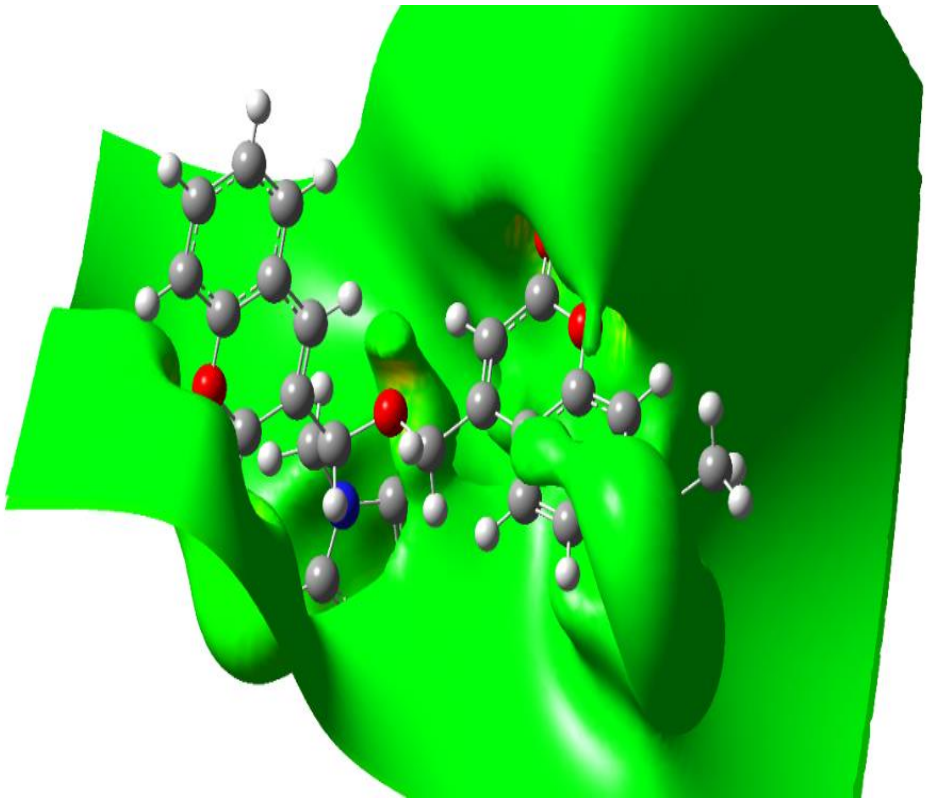

Figure-7 Electrostatic potential mapping of 4BEXO molecule in vacuum

3.3.2. TED of 4BEXO molecule

DFT studies provide a theoretical framework to estimate the total electronic density (TED). Electronic density mapping is used to analyze the molecule's shape, charge, and delocalization, offering insights into its chemical reactivity. Figure 8 illustrates the TED mapping of 4BEXO in vacuum, indicating electronic densities of ±4.077 × 10^{-4} Hartrees (±0.011 eV) in vacuum. The electronic density shows a uniform distribution across the molecule's surface. These results help in

understanding various properties of the system, such as chemical bonding, interactions, and other important electronic properties.

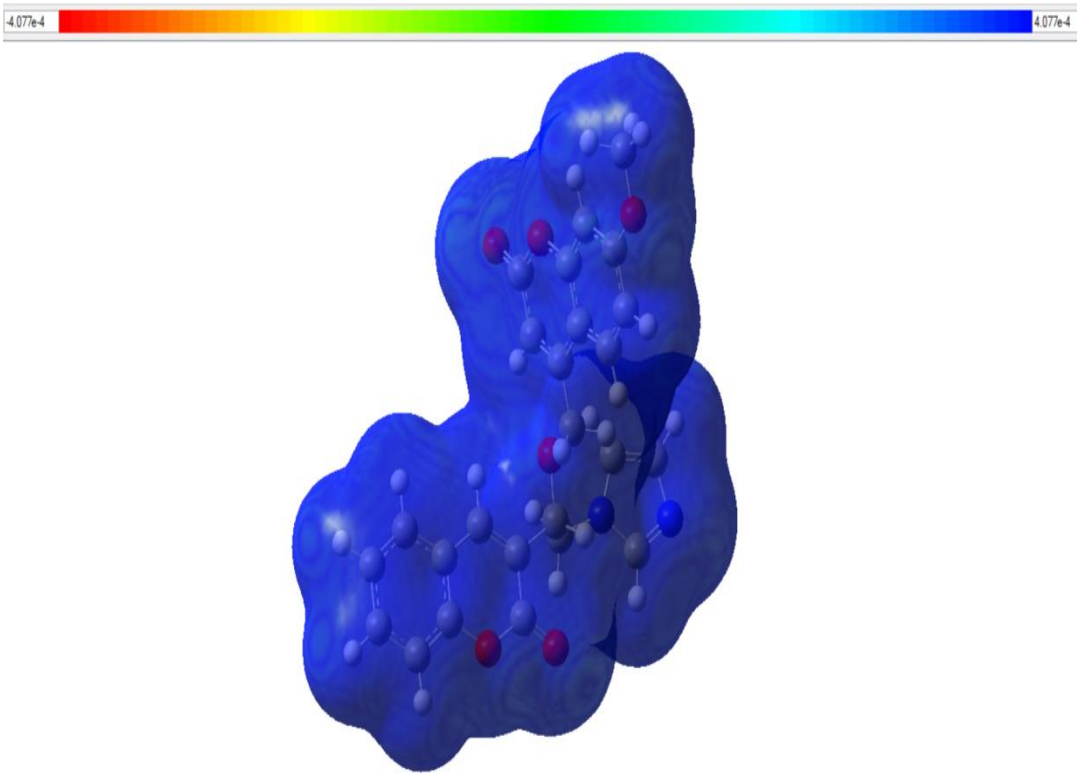

Figure-8 Total electron density mapping of 4BEXO molecule in vacuum

3.3.3. MEP of 4BEXO molecule

The Molecular Electrostatic Potential (MESP) mapping, conducted using DFT/B3LYP/6-311G in various solvents, depicts potential distribution observable by color code. Figure 9 presents the MESP mapping of 4BEXO in vacuum and DMSO, displaying contour values ranging from -7.347 × 10^{-2} eV to 7.347 × 10^{-2} eV in vacuum. The red regions, primarily surrounding atoms O23, O22, O46, O45, and N21, signify lower energy levels, making these atoms susceptible to nucleophilic attacks as electron acceptors. Conversely, the methyl group attached to the carbon atom displays a maximum positive charge (blue region), rendering it susceptible to electrophilic attacks as an electron donor. Yellow color around represents nucleophilic sites. Neutral green regions are widespread across the molecule, particularly in benzene ring structures and certain carbon atoms. Positive charge (light blue) is observed at the position of hydrogen, indicating its role as an electron donor [24].

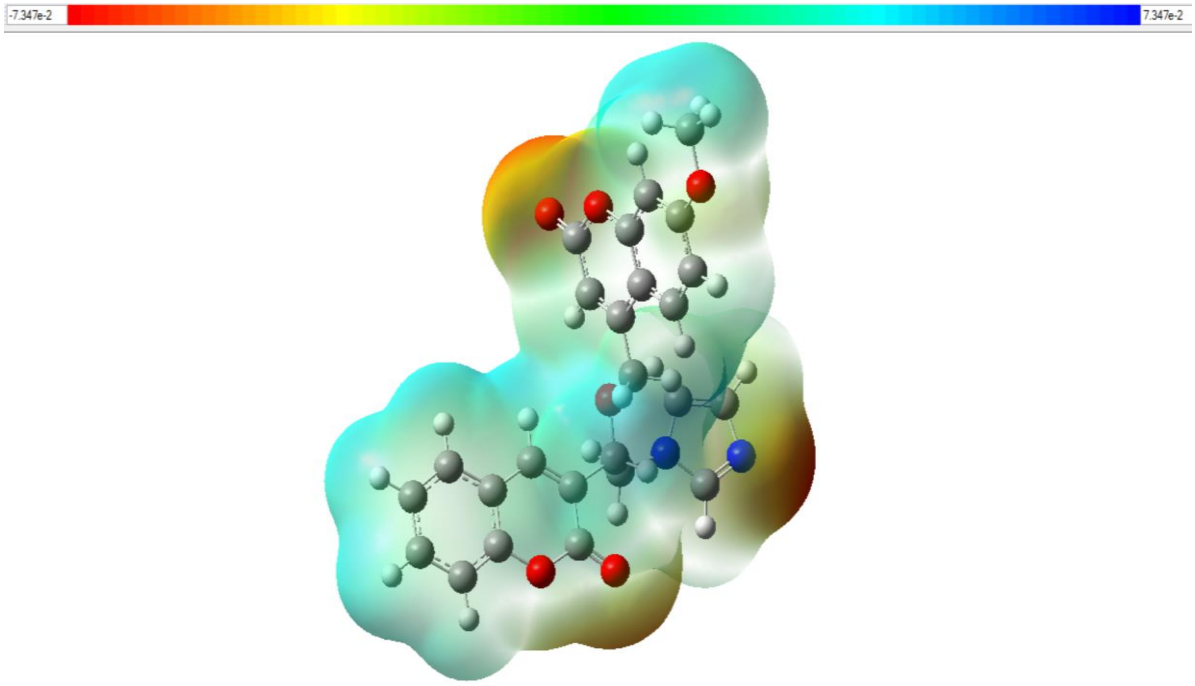

Figure-9 Molecular electrostatic potential mapping of 4BEXO molecule in vacuum

4. Conclusions

This study has effectively utilized a computational approach integrating Density Functional Theory (DFT) and Time-Dependent Density Functional Theory (TD-DFT) to delve into the properties of the 4BEXO molecule. Our analysis of its geometry has unveiled critical structural attributes influencing orbital overlap and charge transfer absorption, underscoring the importance of precise distances and angles. The molecule 4BEXO demonstrates a well-balanced structural and electronic configuration, characterized by stable bond lengths and angles that minimize strain. The Mulliken charge distribution analysis reveals the molecule's adaptability in various solvents, suggesting its versatility in different chemical environments. The Global Chemical Reactivity Descriptors (GCRD) further support its potential for practical applications, with a moderate HOMO-LUMO energy gap indicating stability and reactivity. The molecule's ionization potential, electron affinity, and high electrophilicity index underscore its ability to participate in electron transfer processes, making it suitable for interactions with nucleophiles and other reactive species. Overall, the findings highlight this molecule's potential for diverse applications in chemical and industrial processes, driven by its unique combination of stability, reactivity, and adaptability.

Acknowledgement

We thank DST-FIST lab, Maharani Science College for Women, Bangalore, for the support during the work.

Reference

1. Shareef, S., Rahman, H., & Khan, M. M. (2019). Aminocoumarins: A privileged precursor for the synthesis of fused heterocycles. *Current Organic Chemistry*, *23*(9), 1045-1075.
2. Wei, X., Raj, A. M., Ji, J., Wu, W., Veerakanellore, G. B., Yang, C., & Ramamurthy, V. (2019). Reversal of regioselectivity during photodimerization of 2-anthracenecarboxylic acid in a water-soluble organic cavitand. *Organic Letters*, *21*(19), 7868-7872.

3. Geiger, T., Haupt, A., Maichle-Mössmer, C., Schrenk, C., Schnepf, A., & Bettinger, H. F. (2019). Synthesis and photodimerization of 2-and 2, 3-disubstituted anthracenes: influence of steric interactions and London dispersion on diastereoselectivity. The Journal of Organic Chemistry, 84(16), 10120-10135.
4. Mohr, L. M., Bauer, A., Jandl, C., & Bach, T. (2019). Visible light-mediated intermolecular [2+ 2] photocycloaddition of 1-aryl-2-nitroethenes and olefins. Organic & Biomolecular Chemistry, 17(30), 7192-7203.
5. Zabradnik, M. (1992). The production and application of fluorescent brightening agents. New York, NY: John Wiley & Sons.
6. Heravi, M. M., Sadjadi, S., Oskooie, H. A., Shoar, R. H., & Bamoharram, F. F. (2008). The synthesis of coumarin-3-carboxylic acids and 3-acetyl-coumarin derivatives using heteropolyacids as heterogeneous and recyclable catalysts. Catalysis Communications, 9(3), 470-474.
7. Lin, S., Kuo, P., & Yang, D. (2007). Design and synthesis of a coumarin-based acidichromic colorant. Molecules, 12(7), 1316-1324.
8. Ray, D., & Bharadwaj, P. K. (2008). A coumarin-derived fluorescence probe selective for magnesium. Inorganic Chemistry, 47(6), 2252-2254.
9. Hung, T. T., Lu, Y. J., Liao, W. Y., & Huang, C. L. (2007). Blue violet laser write-once optical disk with coumarin derivative recording layer. IEEE Transactions on Magnetics, 43(2), 867-869.
10. Mukhatar, S., Mujeebur, R. V. P., Ansari, W. H., Lemiere, G., de Groot, A., &Dommisse, R. (1999). Bifunctional derivative of p,p'-dichlorochalcone. Part II. Synthesis of a novel compound 2-[2-Carboxymethylthio-2-(4-chlorophenyl)ethyl]-2-(4-chlorophenyl)-4-thiazolidinone. Molecules, 4(2), 232-237.
11. Milan, C., Maja, M., Tomislav, B., Nela, D., & Valentina, R. (2009). Design and synthesis of some thiazolidin-4-ones based on (7-hydroxy-2-oxo-2H-chromen-4-yl) acetic acid. Molecules, 14(7), 2501-2513.
12. Murraya, R., & Jorge, Z. (1984). A simple method for differentiating between angular and linear 5-methoxyfurano coumarins. Phytochemistry, 23(3), 697-699.
13. Chavan, S., Shivasankara, K., Sivappa, R., & Kale, R. (2002). Zinc-mediated transesterification of β-ketoesters and coumarin synthesis. Tetrahedron Letters, 43(43), 8583-8586.
14. Shapiro, S., & Sherwin, B. (1943). Thromboembolization. II. The use of dicumarol (3,3'-methylenebis(4-hydroxycoumarin)) in embolization: Report of five cases. New York State Journal of Medicine, 43(1), 45-52.
15. Butsch, W. L., & Stewart, J. D. (1942). Administration of dicoumarin compound for prophylaxis of postoperative thrombosis and embolism. Archives of Surgery, 45(4), 551-553.
16. Savanur, H. M., Pawashe, G. M., Kim, K. M., & Kalkhambkar, R. G. (2018). Synthesis and molecular modeling studies of coumarin- and 1-aza-coumarin-linked miconazole analogues and their antifungal activity. Chemistry Select, 3(33), 9648-9653.
17. M.J. Frisch, G.W. Trucks, H.B. Schlegel, G.E. Scuseria, M.A. Robb, J.R. Cheeseman, G. Scalmani, V. Barone, B. Mennucci, G.A. Petersson, H. Nakatsuji, M. Caricato, X. Li, H.P. Hratchian, A.F. Izmaylov, J. Bloino, G. Zheng, J.L. Sonnenberg, M. Hada, M. Ehara, K. Toyota, R. Fukuda, J. Hasegawa, M. Ishida,T. Nakajima, Y. Honda, O. Kitao, H. Nakai, T. Vreven, J.A. Montgomery Jr., J.E. Peralta, F. Ogliaro, M. Bearpark, J.J. Heyd, E. Brothers, K.N. Kudin, V.N. Staroverov, T. Keith, R. Kobayashi, J. Normand, K. Raghavachari, A. Rendell, J.C. Burant, S.S. Iyengar, J. Tomasi, M. Cossi, N. Rega, J.M. Millam,. Klene, J.E. Knox, J.B. Cross, V. Bakken, C. Adamo, J. Jaramillo, R. Gomperts, R.E. Stratmann, O. Yazyev, A.J. Austin, R. Cammi, C. Pomelli, J.W. Ochterski, R.L. Martin, K. Morokuma, V.G. Zakrzewski, G.A. Voth, P. Salvador, J.J. Dannenberg, S. Dapprich, A.D. Daniels, O. Farkas, J.B. Foresman, J.V. Ortiz, J. Cioslowski, D.J. Fox, Gaussian-09, Revision B.01, Gaussian, Inc, Wallingford, CT, 2010

18. Raghavachari, K. Perspect. “Density functional thermochemistry. III. The role of exact exchange” - Becke AD J. Chem. Phys. 98, (2000).
19. Shirley, W. A., Hoffmann, R., & Mastryukov, V. S. (1995). An approach to understanding bond length/bond angle relationships. The Journal of Physical Chemistry, 99(12), 4025-4033.
20. Tsuzuki, S., Uchimaru, T., Tanabe, K., & Yliniemela, A. (1996). Comparison of atomic charge distributions obtained from different procedures: basis set and electron correlation effects. Journal of Molecular Structure: Theochem, 365(2-3), 81-88.
21. Petrushenko, I. K. (2018). Physical Adsorption of N-containing Heterocycles on Hexagonal Boron Nitride: DFT-D3 Study. Journal of Nano-and Electronic Physics, 10(2).
22. Zara, Z., Iqbal, J., Ayub, K., Irfan, M., Mahmood, A., Khera, R. A., & Eliasson, B. (2017). A comparative study of DFT calculated and experimental UV/Visible spectra for thirty carboline and carbazole based compounds. Journal of Molecular Structure, 1149, 282-298.
23. Nogueira, J. J., & González, L. (2018). Computational Photophysics in the Presence of an Environment. Annual Review of Physical Chemistry, 69, 473-497.
24. Tichnell, C. R., Shultz, D. A., Popescu, C. V., Sokirniy, I., & Boyle, P. D. (2015). Synthesis, characterization, and photophysical studies of an iron (III) catecholate–nitronylnitroxide spin-crossover complex. Inorganic Chemistry, 54(9), 4466-4474.